

Inclusive J/ψ Production In Υ Decay Via Color-singlet Mechanism

Zhi-Guo He^{1,2} and Jian-Xiong Wang¹

¹*Institute of High Energy Physics, Chinese Academy of Science,
P.O. Box 918(4), Beijing, 100049, China.*

Theoretical Physics Center for Science Facilities, (CAS) Beijing, 100049, China.

²*Departament d'Estructura i Constituents de la Matèria and Institut de Ciències del Cosmos
Universitat de Barcelona*

*Diagonal, 647, E-08028 Barcelona, Catalonia, Spain.**

(Dated: November 8, 2018)

Abstract

We reconsider the tree level color-singlet contribution for the inclusive J/ψ production in Υ decay with the α_s^5 order QCD process $\Upsilon \rightarrow J/\psi + c\bar{c} + g$ and $\alpha^2 \alpha_s^2$ order QED processes $\Upsilon \rightarrow \gamma^* \rightarrow J/\psi + c\bar{c}$ and $\Upsilon \rightarrow J/\psi + gg$. It is found that the contribution of the QED process is compatible with that of the QCD process, and the numerical results for the QCD process alone is an order of magnitude smaller than the previous theoretical predictions, and our theoretical prediction in total is about an order of magnitude smaller than the recent CLEO measurement on the branching fraction $\mathcal{B}(\Upsilon \rightarrow J/\psi + X)$. It indicates that the J/ψ production mechanism in Υ decay is not well understood, and further theoretical work and experimental analysis are still necessary.

PACS numbers: 12.38.Bx, 12.39.Jh, 13.20.Gd

* Present address

I. INTRODUCTION

Since the discovery of $c\bar{c}$ state J/ψ and $b\bar{b}$ state Υ more than three decades ago, heavy-quarkonium system has served as a good laboratory for testing QCD from both perturbative and non-perturbative aspects. With the accumulation of new experimental data and the development of interesting theory, considerable attention has been attracted to study heavy-quarkonium spectrum, decay and production (for a review see [1]).

On the theoretical side, the non-relativistic QCD(NRQCD)[2] effective field theory was introduced, based on which the production and decay of heavy quarkonium can be calculated with a rigorous factorization formalism. This formalism separates the physics on the energy scale larger than the quark mass m_Q , related to the annihilation or production of $Q\bar{Q}$ pair, from the physics on the scale of $m_Q v^2$ order, relevant to the formation of the bound state. Consequently, the inclusive production and decay rates of heavy quarkonium are factorized into the product of short-distance coefficients, which could be calculated perturbatively as the expansion of α_s , and the corresponding long-distance matrix elements, which are determined by some non-perturbative methods. The long-distance matrix elements are weighted by the powers of v , the velocity of heavy quark in the rest frame of the bound state. One important feature of NRQCD is that it allows the contribution of $Q\bar{Q}$ pair in color-octet configuration in short distance, and the color-octet state will subsequently evaluate into physics state through the emission of soft gluons.

The introduction of NRQCD has greatly improved our understanding of the production mechanism of heavy quarkonium. One remarkable success of NRQCD is that the transverse momentum (p_t) distributions of J/ψ and ψ' production at Fermilab Tevatron[3] could be well described by the color-octet mechanism[4]. However, this mechanism could not correctly explain the CDF measurements of J/ψ polarization[5]. Just about one or two years ago, the next-to-leading order (NLO) QCD corrections to both the color-singlet and color-octet processes have been obtained. For the color-octet process[6], it is found that the leading order (LO) results are little changed when the NLO QCD corrections are taken into account. In the color-singlet case, the theoretical predictions at QCD NLO are significantly changed from the LO results on the p_t distribution and polarization of J/ψ [7]. Although this still could not resolve the puzzle. The large impact of the color-singlet NLO QCD corrections on the LO results indicates that the contribution of the color-octet mechanism may not

as important as we expected before. Furthermore, the theoretical predictions[8] for the p_t distribution of Υ can be compatible with the data of Υ production at Tevatron[9] within the theoretical uncertainty when considering some of the important next-to-next-to-leading-order (NNLO) α_s^5 contribution. However, it still cannot explain the recent polarization measurement by D0 Collaboration [10]

In the case of J/ψ production in e^+e^- annihilation, the existence of color-octet mechanism also faces to a challenge. The NRQCD approach predicts that the J/ψ production in e^+e^- annihilation at LO in α_s is dominated by $e^+e^- \rightarrow J/\psi + gg$, and $e^+e^- \rightarrow J/\psi + c\bar{c}$ and $e^+e^- \rightarrow J/\psi + g$, in which the first two are color-singlet subprocesses and the last one is color-octet subprocess. The color-octet contribution[11] predicts there is a peak in J/ψ momentum spectrum near the kinematic end point. Unfortunately, The peak was not found in the experimental observation of BABAR[12] and Belle[13]. By using the soft-collinear effective theory (SCET), the color-octet predictions[14] could be softened, but it depends on a unknown non-perturbative shape function. Belle also extended their analysis by deriving associated J/ψ production with $c\bar{c}$ pair from inclusive J/ψ production production[15]. The NLO QCD calculations shown that both $\sigma[e^+e^- \rightarrow J/\psi + c\bar{c} + X]$ [16, 17] and $\sigma[e^+e^- \rightarrow J/\psi + X_{\text{non-}c\bar{c}}]$ [18, 19] may be explained by considering only the contribution of color-singlet process. However, it point out in Ref. [17] that the color-octet contribution is still not yet completely ruled out due to the incomplete measurement in the experimental analysis.

To improve our understanding of J/ψ production mechanism, it was proposed[20, 21] that the Υ decay may provide an alternate probe of J/ψ production in rich gluon environment. Experimentally, the branching ratio of $\Upsilon \rightarrow J/\psi + X$ has already been reported to be $(1.1 \pm 0.4 \pm 0.2) \times 10^{-3}$ by CLEO based on about 20 events in Ref.[22]. The ARGUS Collaboration obtained an upper limit of 0.68×10^{-3} [23] at 90% confidence level. With about 35 times larger data sample than previous work, an improved measurement of J/ψ branching ratio and momentum spectrum have been obtained recently by CLEO Collaboration with $\mathcal{B}(\Upsilon \rightarrow J/\psi + X) = (6.4 \pm 0.4 \pm 0.6) \times 10^{-4}$ [24]. Theoretically, the color-octet prediction is $\mathcal{B}(\Upsilon \rightarrow J/\psi + X) \simeq 6.2 \times 10^{-4}$ [21] with 10% contribution from $\psi(2S)$ feed-down and another 10% from χ_{cJ} [25]. However, it was found that the branching ratio of color-singlet process $\Upsilon \rightarrow J/\psi + c\bar{c}g$ is about 5.9×10^{-4} [26], which is also in agreement with experimental measurement. Although both the color-singlet and color-octet decay modes may explain the total decay rate independently, their predictions on the J/ψ momentum spectrum are

significantly different. The maximum value of J/ψ momentum in the color-singlet and color-octet process are 3.7 GeV and 4.5 GeV respectively. The CLEO collaboration found that the experimental result of J/ψ momentum spectrum is much softer than color-octet predictions and somewhat softer than color-singlet predictions. The process $\Upsilon \rightarrow J/\psi + X$ also was studied in color evaporation model[27] more than thirty years ago, but this model can not give systematic predictions of J/ψ production. Another early theoretical work on the process $\Upsilon \rightarrow J/\psi + X$ could be found in Ref.[28].

There is a very well agreement between the LO color-singlet predictions[26] and experimental measurements[24]. But it seems difficult to understand the situation in comparison with the case of the J/ψ production at B factories, where there are huge discrepancies between the LO theoretical predictions and the experimental measurements. Therefore, we re-calculate the branching ratio of color-singlet process $\Upsilon \rightarrow J/\psi + c\bar{c} + g$ in this paper. And the results show that it is an order of magnitude smaller than the previous theoretical prediction [26]. Therefore, there is an order of magnitude discrepancy between the LO theoretical prediction and experimental measurement for $\Upsilon \rightarrow J/\psi + X$ now. To further clarify the situation, we also estimate the leading-order contribution of the QED processes $\Upsilon \rightarrow \gamma^* \rightarrow J/\psi + c\bar{c}$ and $\Upsilon \rightarrow J/\psi + gg$ at $\alpha^2\alpha_s^2$ order, in which the process $\Upsilon \rightarrow J/\psi + gg$ includes two gauge invariant subsets, $\Upsilon \rightarrow \gamma^* \rightarrow J/\psi + gg$ and $\Upsilon \rightarrow \gamma^*gg$ followed by $\gamma^* \rightarrow J/\psi$. The final results show that the contribution from the QED processes are compatible with that from the QCD process.

The rest of paper is organized as follows: In section II, the basic formula and method used in the calculation are presented. In section III, we describe the calculation on the branching ratio of the QCD process $\Upsilon \rightarrow J/\psi + c\bar{c} + g$ and J/ψ momentum spectrum. In section IV, we estimate the contribution of the two QED processes $\Upsilon \rightarrow J/\psi + c\bar{c}$ and $\Upsilon \rightarrow J/\psi + gg$. The final results and summary are given in the last section.

II. DESCRIPTION OF OUR BASIC CALCULATION FORMULA

At leading order in v_Q , for S-wave heavy-quarkonium production and decay, the color-singlet model predictions are equal to that based on NRQCD effective theory. Then we express $d\Gamma(\Upsilon \rightarrow J/\psi + X)$ as:

$$d\Gamma(\Upsilon \rightarrow J/\psi + X) = d\hat{\Gamma}(b\bar{b}[^3S_1, \underline{1}] \rightarrow c\bar{c}[^3S_1, \underline{1}] + X) \langle \Upsilon | \mathcal{O}_1(^3S_1) | \Upsilon \rangle \langle \mathcal{O}_1^\psi(^3S_1) \rangle, \quad (1)$$

where $d\Gamma(b\bar{b}[{}^3S_1, \underline{1}] \rightarrow c\bar{c}[{}^3S_1, \underline{1}] + X)$ represents color-singlet $b\bar{b}$ pair in spin-triplet state decay into color-singlet $c\bar{c}$ pair in spin-triplet state with anything, which is calculated perturbatively, and $\langle \Upsilon | \mathcal{O}_1({}^3S_1) | \Upsilon \rangle$ and $\langle \mathcal{O}_1^\psi({}^3S_1) \rangle$ are the long-distance matrix elements, which can be related to the nonrelativistic wave functions as:

$$\langle \Upsilon | \mathcal{O}_1({}^3S_1) | \Upsilon \rangle \simeq \frac{3}{2\pi} |R_\Upsilon(0)|^2, \langle \mathcal{O}_1^\psi({}^3S_1) \rangle = \frac{9}{2\pi} |R_\psi(0)|^2. \quad (2)$$

We employ spinor projection method[29] to calculate the short-distance part $d\hat{\Gamma}$. In the nonrelativistic limit, the amplitude of $b\bar{b}[{}^3S_1, \underline{1}] \rightarrow c\bar{c}[{}^3S_1, \underline{1}] + X$ could be written as[30]:

$$\begin{aligned} \mathcal{M}(b\bar{b}[{}^3S_1, \underline{1}](p_0) \rightarrow c\bar{c}[{}^3S_1, \underline{1}](p_1) + X) &= \sum_{s_1, s_2} \sum_{i, l} \sum_{s_3, s_4} \sum_{k, l} \\ &\times \langle s_1; s_2 | 1S_z \rangle \langle 3i; \bar{3}j | 1 \rangle \times \langle s_3; s_4 | 1S_z \rangle \langle 3k; \bar{3}l | 1 \rangle \\ &\times \mathcal{M}(b_i(\frac{p_0}{2}, s_1) \bar{b}_j(\frac{p_0}{2}, s_2) \rightarrow c_k(\frac{p_1}{2}, s_3) \bar{c}_l(\frac{p_1}{2}, s_4) + X) \end{aligned} \quad (3)$$

where $\langle 3i; \bar{3}j | 1 \rangle = \delta_{ij}/\sqrt{N_c}$, $\langle 3k; \bar{3}l | 1 \rangle = \delta_{kl}/\sqrt{N_c}$, $\langle s_1; s_2 | 1S_z \rangle$, and $\langle s_3; s_4 | 1S_z \rangle$ are the SU(3)-color, SU(2)-spin and angular momentum Clebsch-Gordan (C-G) coefficients for $Q\bar{Q}$ projecting on certain appropriate configurations at short distance. At leading order in $v_Q(Q = b, c)$, the projection of spinors $u(\frac{p_0}{2}, s_1)\bar{v}(\frac{p_0}{2}, s_2)$ and $v(\frac{p_1}{2}, s_3)\bar{u}(\frac{p_1}{2}, s_4)$ could be expressed as:

$$\Pi_b = \sum_{s_1, s_2} \langle s_1; s_2 | 1S_z \rangle u(\frac{p_0}{2}, s_1) \bar{v}(\frac{p_0}{2}, s_2) = \frac{1}{2\sqrt{2}} \epsilon(S_z) (\not{p}_0 - 2m_b), \quad (4a)$$

$$\Pi_c = \sum_{s_1, s_2} \langle s_1; s_2 | 1S_z \rangle v(\frac{p_1}{2}, s_3) \bar{u}(\frac{p_1}{2}, s_4) = \frac{1}{2\sqrt{2}} \epsilon(S_z) (\not{p}_1 + 2m_c), \quad (4b)$$

where $\epsilon(S_z)$ is the polarization vector of the heavy quarkonium. For a spin=1 state with momentum p , the sum over its all possible states S_z is

$$\sum_{S_z} \epsilon_\alpha(S_z) \epsilon_\beta^*(S_z) = (-g_{\alpha\beta} + \frac{p_\alpha p_\beta}{p^2}) \quad (5)$$

According to the spinor projection method, the relation between $d\hat{\Gamma}$ and $|\mathcal{M}|^2$ for the $b\bar{b}[{}^3S_1, \underline{1}] \rightarrow c\bar{c}[{}^3S_1, \underline{1}] + X$ is

$$d\hat{\Gamma}(b\bar{b}[{}^3S_1, \underline{1}] \rightarrow c\bar{c}[{}^3S_1, \underline{1}] + c\bar{c} + g) = \frac{1}{3} \frac{1}{4m_b} \frac{1}{3m_b m_c} \frac{\sum |\mathcal{M}|^2}{(2N_c)^2} d\Phi_n \quad (6)$$

where \sum means to sum over all possible polarization states of the particles in this process and Φ_n is the n-body phase space. The factor $(1/2N_c)^2$ with $N_c = 3$ comes from the normalization factor of the NRQCD 4-Fermion operator.

Since our calculation gives different results from the previous theoretical prediction [26], we further checked our results by using two different way to do all the calculations. One is to apply the above formula to write a piece of program to do the calculations for each process described in the following two section. Another is just using the Feynman Diagram Calculation (FDC) Package [31] to generate all the needed Fortran source and then do the numerical calculation. We obtained exactly the same results by using these two methods. Moreover, to check gauge invariance, in the expression of FDC version source, the gluon polarization vector is explicit kept and then is replaced by its 4-momentum in the final numerical calculation. Definitely the result must be zero and our results confirm it.

III. THE QCD PROCESS $\Upsilon \rightarrow J/\psi + c\bar{c} + g$

Now we proceed to calculate the total decay rate of $\Upsilon \rightarrow J/\psi + c\bar{c} + g$ and its contribution to the J/ψ momentum spectrum. At leading order in α_s , there are six Feynman diagrams which are shown in Fig. 1. The amplitude \mathcal{M} could be factorized as:

$$\begin{aligned} \mathcal{M}(b\bar{b}[^3S_1, \underline{1}](p_0) \rightarrow c\bar{c}[^3S_1, \underline{1}](p_1) + c(p_2)\bar{c}(p_3) + g(p_4)) = \\ \mathcal{M}_b(b\bar{b}[^3S_1, \underline{1}] \rightarrow g^*g^*g) \times \mathcal{M}_c(g^*g^* \rightarrow c\bar{c}[^3S_1, \underline{1}] + c\bar{c}), \end{aligned} \quad (7)$$

in which the later one is universal for all the six diagrams and it is

$$\mathcal{M}_c = \frac{g_s^2}{(p_2 + p_1/2)^2(p_3 + p_1/2)^2} \bar{u}(p_2)\gamma^\mu \Pi_c \gamma^\nu v(p_3). \quad (8)$$

The amplitude of $\mathcal{M}_b(b\bar{b}[^3S_1, \underline{1}] \rightarrow g^*g^*g)$, for example for the first diagram, is

$$\mathcal{M}_b^1 = g_s^3 C_1 \text{Tr}[\Pi_b \gamma^\mu \frac{-\not{p}_0 + \not{p}_1 + \not{p}_3 + m_b}{(-p_0/2 + p_1/2 + p_3)^2 - m_b^2} \gamma^\nu \frac{\not{p}_0 - \not{p}_4 + m_b}{(p_0/2 - p_4)^2 - m_b^2} \not{\epsilon}_3] \quad (9)$$

where C_1 is the corresponding color coefficient and $\not{\epsilon}_3$ is the polarization vector of the real gluon. The amplitude \mathcal{M}_b^i for the other five diagrams could be obtained in a similar way. An analytical expression of $\sum |\mathcal{M}|^2$ is obtained in the calculation, but is too lengthy to be presented here.

The four-body phase space Φ_4 for $b\bar{b}[^3S_1, \underline{1}] \rightarrow c\bar{c}[^3S_1, \underline{1}] + c\bar{c} + g$ is defined as

$$d\Phi_4(p_0 \rightarrow p_1 + p_2 + p_3 + p_4) = \prod_{k=1}^4 \frac{d^3\vec{p}_k}{(2\pi)^3 2E_k} (2\pi)^4 \delta^4(p_0 - \sum_{k=1}^4 p_k) \quad (10)$$

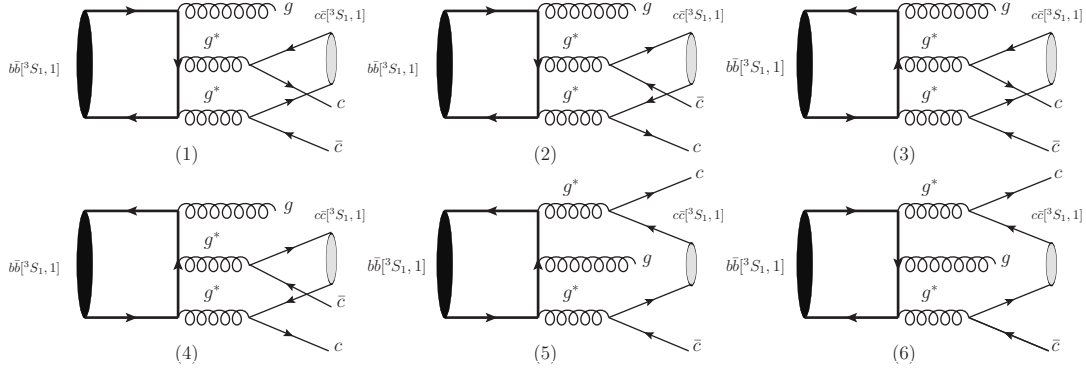


FIG. 1: The six Feynman diagrams for the short-distance process: $b\bar{b}[{}^3S_1, 1] \rightarrow c\bar{c}[{}^3S_1, 1] + c\bar{c} + g$.

There are many ways to perform the four-body phase-space integration. Here we briefly introduce our methods. Using the two following identical equation

$$\int \frac{d^4 p_{234}}{(2\pi)^4} (2\pi)^4 \delta^4(p_{234} - p_2 - p_3 - p_4) \equiv 1, \quad \int \frac{d^4 p_{34}}{(2\pi)^4} (2\pi)^4 \delta^4(p_{34} - p_3 - p_4) \equiv 1, \quad (11)$$

we transform the four-body space into the combination of three two-body phase spaces, which is given by

$$d\Phi_4(p_0 \rightarrow p_1 + p_2 + p_3 + p_4) = \frac{ds_{234}}{2\pi} \frac{ds_{34}}{2\pi} d\Phi_2(p_0 \rightarrow p_1 + p_{234}) d\Phi_2(p_{234} \rightarrow p_2 + p_{34}) d\Phi_2(p_{34} \rightarrow p_3 + p_4) \quad (12)$$

where $s_{234} = p_{234}^2$, $s_{34} = p_{34}^2$. The three two-body phase spaces integration are described by the three-momenta $\vec{p}_1, \vec{p}_2^*, \vec{p}_3^{**}$ and their solid angle element $d\Omega_0, d\Omega_{234}^*, d\Omega_{34}^{**}$ in the rest frames of p_0, p_{234} , and p_{34} respectively. Then the expression of four-body phase space becomes

$$d\Phi_4 = \int \frac{ds_{234}}{2\pi} \int \frac{|\vec{p}_1|}{8(2\pi)^2 m_b} d\Omega_0 \int \frac{ds_{34}}{2\pi} \int d\Omega_{234}^* \frac{|\vec{p}_2^*|}{4(2\pi)^2 \sqrt{s_{234}}} \int \frac{|\vec{p}_3^{**}|}{4(2\pi)^2 \sqrt{s_{34}}} d\Omega_{34}^{**}. \quad (13)$$

where $|\vec{p}_1|$, $|\vec{p}_2^*|$ and $|\vec{p}_3^{**}|$ are given in the equations below in the rest frame of p_0, p_{234} and p_{34} respectively

$$|\vec{p}_1| = \frac{\sqrt{16m_b^4 + (-4m_c^2 + s_{234})^2 - 8m_b^2(4m_c^2 + s_{234})}}{4m_b} \quad (14a)$$

$$|\vec{p}_2^*| = \frac{\sqrt{(s_{234} - (m_c - \sqrt{s_{34}})^2)(s_{234} - (m_c + \sqrt{s_{34}})^2)}}{2\sqrt{s_{234}}} \quad (14b)$$

$$|\vec{p}_3^{**}| = \frac{s_{34} - m_c^2}{2\sqrt{s_{34}}} \quad (14c)$$

TABLE I: The values of $f(r)$ for different $r = m_c/m_b$

r	0.275	0.296	0.317	0.327	0.338	0.361	0.381
f(r)	0.904	0.567	0.345	0.269	0.202	0.105	0.055

The integration ranges of s_{234} and s_{34} are

$$4m_c^2 < s_{234} < (2m_b - 2m_c)^2, m_c^2 < s_{34} < (\sqrt{s_{234}} - m_c)^2. \quad (15)$$

For space-symmetry, $d\Omega_0$ and $d\phi_{234}^*$ could be integrated out directly then $|\mathcal{M}|^2$ only dependent on five variables s_{234} , s_{34} , θ_{234}^* , θ_{34}^{**} , and ϕ_{34}^{**} . To get the total decay rate, the non-trivial integral with these five variables is performed by three steps. First, we do the integration $d\Omega_{34}^{**}$ in the rest frame of p_{34} , then we integrate out s_{34} and θ_{234}^* in the rest frame of p_{234} , the last variable s_{234} is integrated out in Υ rest frame. Since $|\vec{p}_1|$ only depend on s_{234} , the J/ψ momentum spectrum could be easily obtained by replacing ds_{234} with $\frac{ds_{234}}{d|\vec{p}_1|}d|\vec{p}_1|$. The phase space integrations for the total rate and J/ψ momentum spectrum are calculated numerically.

By dimension analysis, it is easy to represent the decay width and differential decay width of $\Upsilon \rightarrow J/\psi + c\bar{c} + g$ as

$$\Gamma(\Upsilon \rightarrow J/\psi + c\bar{c} + g) = \frac{\alpha_s^5}{m_b^5} f(r) \frac{\langle \Upsilon | \mathcal{O}_1(^3S_1) | \Upsilon \rangle \langle \mathcal{O}_1^\psi(^3S_1) \rangle}{2N_c \cdot 3 \times 2N_c}. \quad (16a)$$

$$\frac{d\Gamma}{d|\vec{p}_1|}(\Upsilon \rightarrow J/\psi + c\bar{c} + g) = \frac{\alpha_s^5}{m_b^5} g(r, |\vec{p}_1|/m_b) \frac{\langle \Upsilon | \mathcal{O}_1(^3S_1) | \Upsilon \rangle \langle \mathcal{O}_1^\psi(^3S_1) \rangle}{2N_c \cdot 3 \times 2N_c}. \quad (16b)$$

where $r = m_c/m_b$ and $f(r)$ are dimensionless, and $f(r)$ function is same as $h(r)$ in Ref.[26]. To ensure the validity of our calculations, we use two different kinds of computer codes for cross check and obtain exactly the same results for $f(r)$ and $g(r, |\vec{p}_1|/m_b)$. When $r = 0.327$, the decay width is

$$\Gamma(\Upsilon \rightarrow J/\psi + c\bar{c} + g) = \frac{\alpha_s^5}{m_b^5} \frac{\langle \Upsilon | \mathcal{O}_1(^3S_1) | \Upsilon \rangle \langle \mathcal{O}_1^\psi(^3S_1) \rangle}{2N_c \cdot 3 \times 2N_c} \times 0.269. \quad (17)$$

To compare our results with those in Ref. [26], the numerical results of $f(r)$ in the range of $0.275 \leq r \leq 0.381$ are listed in Tab.[I]. It is easy to see that the results of $f(r)$ are about an order of magnitude smaller than that given in Ref.[26] and $f(r)$ changes a little sharper than that when r goes from 0.275 to 0.381. Besides $f(r)$, the decay width $\Gamma(\Upsilon \rightarrow J/\psi + c\bar{c} + g)$ is also dependent on the choice of the values of the two long-distance matrix

elements $\langle \Upsilon | \mathcal{O}_1(^3S_1) | \Upsilon \rangle, \langle \mathcal{O}_1^\psi(^3S_1) \rangle$, the coupling constant α_s and the mass of b-quark. To reduce the uncertainty of theoretical predictions, we normalize it by the decay width of $\Upsilon \rightarrow$ light hadron, which includes two dominate decay modes $\Upsilon \rightarrow ggg$ and $\Upsilon \rightarrow \gamma^* \rightarrow q\bar{q}$ ($q = u, d, s, c$). At leading order in α_s and v_b , we have

$$\Gamma(\Upsilon \rightarrow ggg) = \frac{20\alpha_s^3(\pi^2 - 9)}{243m_b^2} \langle \Upsilon | \mathcal{O}_1(^3S_1) | \Upsilon \rangle, \quad (18a)$$

$$\Gamma(\Upsilon \rightarrow q\bar{q}) = \frac{2\pi N_c e_q^2 e_b^2 \alpha^2}{m_b^2} \langle \Upsilon | \mathcal{O}_1(^3S_1) | \Upsilon \rangle. \quad (18b)$$

Then the normalized width $\Gamma_{\text{Nor}}^{c\bar{c}g}$ is given by

$$\Gamma_{\text{Nor}}^{c\bar{c}g} = \frac{f(r)\alpha_s^5 \langle \mathcal{O}_1^\psi(^3S_1) \rangle}{3(2N_c)^2 \left(\frac{20}{243} \alpha_s^3 (\pi^2 - 9) + \sum_q 2\pi N_c e_q^2 e_b^2 \alpha^2 \right) m_b^3} \quad (19)$$

and the branching ratio turns to be

$$\mathcal{B}(\Upsilon \rightarrow J/\psi + c\bar{c} + g) = \Gamma_{\text{Nor}}^{c\bar{c}g} \times \mathcal{B}(\Upsilon \rightarrow \text{light hadron}). \quad (20)$$

Since the process $\Upsilon \rightarrow J/\psi + c\bar{c} + g$ can be viewed as $\Upsilon \rightarrow gg^*g^*$ followed by $g^*g^* \rightarrow J/\psi + c\bar{c}$, as suggested in Ref.[20], it is reasonable to chose $\alpha_s(2m_c) = 0.259$. Using $e_u = \frac{2}{3}$, $e_d = -\frac{1}{3}, e_s = -\frac{1}{3}, e_c = \frac{2}{3}$, $e_b = \frac{1}{3}$, $\alpha = \frac{1}{128}$, $r = \frac{1.548}{4.73} \simeq 0.327$, $m_b = 4.73\text{GeV}$, $|R_\psi(0)|^2 = 0.81\text{GeV}^3$ being calculated in potential model[32] and $\mathcal{B}(\Upsilon \rightarrow \text{light hadron}) = 92\%$ [34], we predict

$$\mathcal{B}(\Upsilon \rightarrow J/\psi + c\bar{c} + g) = 2.12 \times 10^{-5} \quad (21)$$

The normalized J/ψ momentum spectrum $d\Gamma_{\text{Nor}}/d|\vec{p}_1|$ is shown in Fig. 3. It is easy to see that the shape of the J/ψ momentum spectrum is similar with that in Ref.[26], although the prediction for the total decay width is an order of magnitude smaller than the experimental data.

IV. THE QED PROCESS $\Upsilon \rightarrow J/\psi + X$

There are two QED processes $\Upsilon \rightarrow J/\psi + c\bar{c}$ and $\Upsilon \rightarrow J/\psi + gg$ at the leading order in α_s and α . Both of them are considered in this work. We will present a few simple steps and analytic results for them in the following.

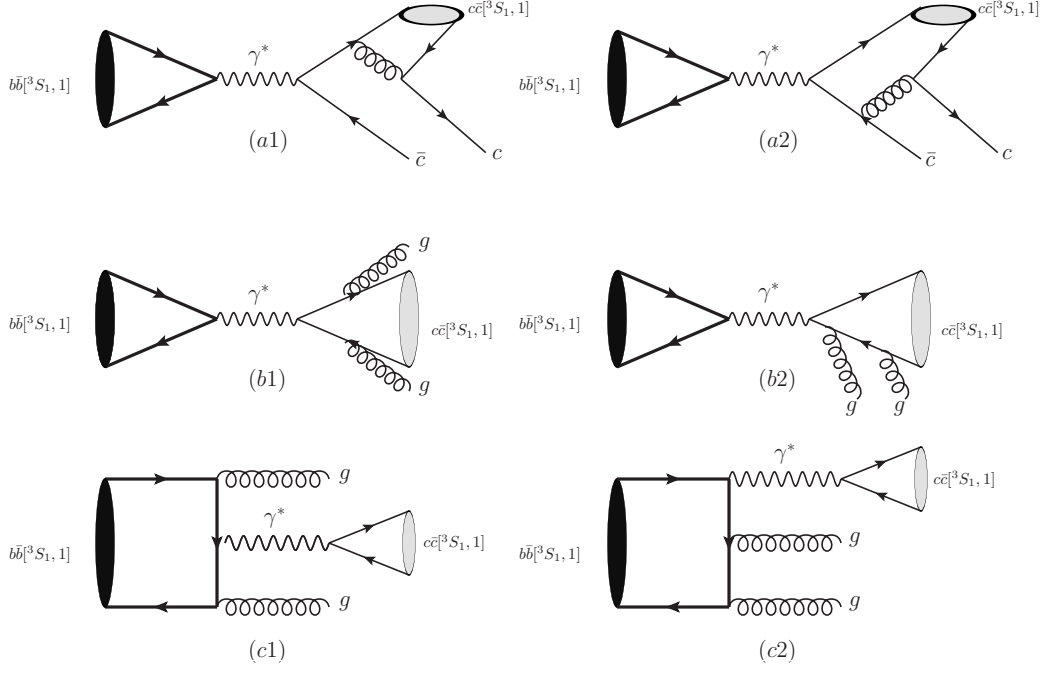


FIG. 2: The typical Feynman diagrams for the QED processes of inclusive J/ψ production: (a) $b\bar{b}[{}^3S_{1,1}] \rightarrow \gamma^* \rightarrow c\bar{c}[{}^3S_{1,1}] + c\bar{c}$, (b) $b\bar{b}[{}^3S_{1,1}] \rightarrow \gamma^* \rightarrow c\bar{c}[{}^3S_{1,1}] + gg$, (c) $b\bar{b}[{}^3S_{1,1}] \rightarrow c\bar{c}[{}^3S_{1,1}] + gg$.

A. $\Upsilon \rightarrow \gamma^* \rightarrow J/\psi + c\bar{c}$

At the leading order, there are four Feynman diagrams for $\Upsilon(p_0) \rightarrow \gamma^* \rightarrow J/\psi(p_1) + c(p_2)\bar{c}(p_3)$, two of which are shown in Fig. 2a. The calculation procedure for this process is very similar to that for the J/ψ production in association with $c\bar{c}$ pair in e^+e^- annihilation. The differential decay width is given by

$$\begin{aligned}
\frac{d\Gamma}{d|\vec{p}_1|}(\Upsilon \rightarrow \gamma^* \rightarrow J/\psi + c\bar{c}) &= \frac{2\pi C_A C_F^2 e_b^2 e_c^2 \alpha^2 \alpha_s^2 \langle \Upsilon | \mathcal{O}_1({}^3S_1) | \Upsilon \rangle \langle \mathcal{O}_1^\psi({}^3S_1) \rangle \sqrt{x_1^2 - 4r^2}}{9(2N_c)^2 m_b^6 r x_1^4 (\kappa - x_1)^3 (-2 + x_1)^2 (\kappa + x_1)^3} \\
&(2\kappa x_1(-2\kappa^6(1 + 2r^2)x_1^2 + \kappa^4(6r^6(-4 + 3x_1^2) + 2x_1^2(-4 + x_1^2(-2 + 9x_1)) - \\
&4r^4(16 + x_1(-16 + x_1(-8 + 9x_1)))) + r^2(-2 + x_1)(16 + x_1(-24 + x_1(-14 + 39x_1)))) + \\
&2\kappa^2 x_1^2(8x_1^2 + 7x_1^4 - 18x_1^5 - 4r^6(-8 + x_1(8 + x_1)) + 4r^4(20 + x_1(-40 + x_1(13 + 4x_1))) + \\
&r^2(32 + x_1(-96 + x_1(60 + (76 - 37x_1)x_1)))) + x_1^4(6r^6(4 + x_1^2) + 2x_1^2(-4 + x_1^2(-4 + 9x_1)) + \\
&4r^4(8 + x_1(32 + (-26 + x_1)x_1)) + r^2(-32 + x_1(128 + x_1(-124 - 60x_1 + 39x_1^2)))))) + \\
&(\kappa - x_1)^3(\kappa + x_1)^3(-6r^6(4 + x_1^2) + 2x_1^2(4 + x_1^2(-13 + 8x_1))4r^4(-16 + x_1 + \\
&(16 + x_1(-4 + 5x_1))) + r^2(-32 + x_1(64 + x_1(4 + (4 - 7x_1)x_1)))) \log \frac{x_1 - \kappa}{x_1 + \kappa}), \tag{22}
\end{aligned}$$

where $C_A = 3$ and $C_F = \frac{4}{3}$ are the color factors, and there are $x_1 = \sqrt{|\vec{p}_1|^2 + 4m_c^2}/m_b$ and $\kappa = \sqrt{(x_1 + 2r)(x_1 - 2r)(1 + r^2 - x_1)(1 - x_1)/(1 + r^2 - x_1)}$.

Integrating $|\vec{p}_1|$ numerically and normalizing $\Gamma(\Upsilon \rightarrow \gamma^* \rightarrow J/\psi + c\bar{c})$ by $\Gamma(\Upsilon \rightarrow \text{light hadron})$, we obtain

$$\Gamma_{\text{Normal}}^{c\bar{c}} = \frac{\Gamma(\Upsilon \rightarrow \gamma^* \rightarrow J/\psi + c\bar{c})}{\Gamma(\Upsilon \rightarrow \text{light hadron})} = \frac{3.85\alpha^2\alpha_s^2\langle\mathcal{O}_1^\psi(^3S_1)\rangle}{6N_c(\frac{20}{243}\alpha_s^3(\pi^2 - 9) + \sum_q 2\pi e_q^2 e_b^2 \alpha^2)m_b^3}. \quad (23)$$

By choosing the same numerical values for r , m_b , e_q , α $\langle\mathcal{O}_1^\psi(^3S_1)\rangle$ and $\mathcal{B}(\Upsilon \rightarrow \text{light hadron})$ as those in Sec.III, the numerical result is

$$\mathcal{B}(\Upsilon \rightarrow \gamma^* \rightarrow J/\psi + c\bar{c}) = 1.06 \times 10^{-6}, \quad (24)$$

and the normalized J/ψ momentum spectrum is shown in Fig. 3.

B. $\Upsilon \rightarrow J/\psi + gg$

The process $\Upsilon(p_0) \rightarrow J/\psi(p_1) + g(p_2)g(p_3)$ includes two parts, $\Upsilon \rightarrow \gamma^* \rightarrow J/\psi + gg$ and $\Upsilon \rightarrow gg\gamma^*$ and $\gamma^* \rightarrow J/\psi$. There are six Feynman diagrams for each part at the leading order with the typical ones shown in Fig. 2b and 2c. To calculate the contribution of the two parts together, the differential decay width is represented as

$$\begin{aligned} \frac{d\Gamma}{d|\vec{p}_1|}(\Upsilon \rightarrow J/\psi + gg) &= \frac{32\pi C_A C_F e_c^2 e_b^2 \alpha^2 \alpha_s^2 \langle\Upsilon|\mathcal{O}_1(^3S_1)|\Upsilon\rangle \langle\mathcal{O}_1^\psi(^3S_1)\rangle \sqrt{x_1^2 - 4r^2}}{9(2N_c)^2 m_b^6 r^3 x_1 (-1 + r^2) (2r^2 - x_1)^3 (-2 + x_1)^3} \\ &((-1 + r)(1 + r)(2r^2 - x_1)(-2 + x_1) \sqrt{-4r^2 + x_1^2} (8 + 8r^8 - 4r^6(-4 + 3x_1) + \\ &r^4(-2 + x_1)(-16 + 7x_1) + x_1(-12 + (7 - 2x_1)x_1) - 2r^2(-1 + x_1)(8 + (-7 + x_1)x_1)) + \\ &2(1 + r^2 - x_1)(-((2r^2 - x_1)(8 + 2r^8 + x_1(-12 + 5x_1) + r^6(40 + x_1(-32 + 5x_1)) + \\ &r^4(6 - (-2 + x_1)x_1(-19 + 6x_1)) + r^2 x_1(-6 + x_1(13 + 2(-5 + x_1)x_1))) \\ &\log(\frac{-2 + x_1 - \sqrt{-4r^2 + x_1^2}}{-2 + x_1 + \sqrt{-4r^2 + x_1^2}})) + r^2(-2 + x_1)(8r^{10} - 12r^8 x_1 + x_1^2(5 + 2(-3 + x_1)x_1) + \\ &r^6(6 + x_1(-6 + 5x_1)) + r^4(40 + x_1(-38 + 13x_1)) + r^2(2 + x_1(-32 + (31 - 10x_1)x_1))) \\ &\log(\frac{-2r^2 + x_1 + \sqrt{-4r^2 + x_1^2}}{-2r^2 + x_1 - \sqrt{-4r^2 + x_1^2}}))), \end{aligned} \quad (25)$$

Where there is $x_1 = \sqrt{|\vec{p}_1|^2 + 4m_c^2}/m_b$. And the normalized decay width becomes

$$\Gamma_{\text{Normal}}^{gg} = \frac{\Gamma(\Upsilon \rightarrow J/\psi + gg)}{\Gamma(\Upsilon \rightarrow \text{light hadron})} = \frac{60.8\alpha^2\alpha_s^2\langle\mathcal{O}_1^\psi(^3S_1)\rangle}{6N_c(\frac{20}{243}\alpha_s^3(\pi^2 - 9) + \sum_q 2\pi e_q^2 e_b^2 \alpha^2)m_b^3}. \quad (26)$$

By using the same parameters as above. We obtain

$$\mathcal{B}(\Upsilon \rightarrow J/\psi + gg) = 1.67 \times 10^{-5} \quad (27)$$

and the normalized J/ψ momentum spectrum is plotted in Fig. 3. In the numerical result, about 85.2% contribution comes from the $\Upsilon \rightarrow gg\gamma^*(J/\psi)$ part, 18.2% from the $\Upsilon \rightarrow \gamma^* \rightarrow J/\psi gg$ part and -3.4% from the interference part.

V. SUMMARY AND DISCUSSION

To sum up all the contributions of the color-singlet QED and QCD processes considered above, the branching ratio of direct J/ψ production in Υ decay is

$$\mathcal{B}_{\text{Direct}}(\Upsilon \rightarrow J/\psi + X) = 3.9 \times 10^{-5}, \quad (28)$$

and the corresponding normalized J/ψ momentum distribution is given by the solid line in Fig. 3. It can be seen in Fig. 3 that the contribution of the QCD process is dominated in small p_ψ region, while the effect of the QED process $J/\psi + gg$ is more important in large p_ψ region. In Eq. (25) and the dot-dashed line in Fig. 3, the logarithmic divergence at the kinematic end point is obvious shown for the QED process $J/\psi + gg$. It was pointed out in Ref [14, 18, 33] that both the α_s and v_b expansion failed near the kinematic end point region in the similar processes $e^+e^- \rightarrow J/\psi + X$ and $\Upsilon \rightarrow \gamma + X$ because of the large perturbative and non-perturbative corrections, and the logarithmic divergent behavior can be softened by applying the resummation in the SCET. Whatever it can improve the J/ψ momentum spectrum largely near the kinematic end point, but the corrections to the total decay width is small. Therefore we omit the resummation effect here.

Our calculations show that at the leading order in α_s , v_b and v_c , the QCD process $\Upsilon \rightarrow J/\psi + c\bar{c} + g$ only accounts for 54.4% of the LO theoretical prediction for total branching ratio, in spite of an enhancement factor α_s^3/α^2 that is associated with the QCD and QED coupling constants when compared to the QED processes. The main reason lies on the fact that the virtuality of the two virtual gluons are both of m_b^2 order in the QCD process while the virtuality of the photon is fixed to $4m_c^2$ in the QED processes dominated by $\Upsilon \rightarrow gg\gamma^*(J/\psi)$, and moreover the four-body phase space of the QCD process is also less than the three-body one of the QED processes.

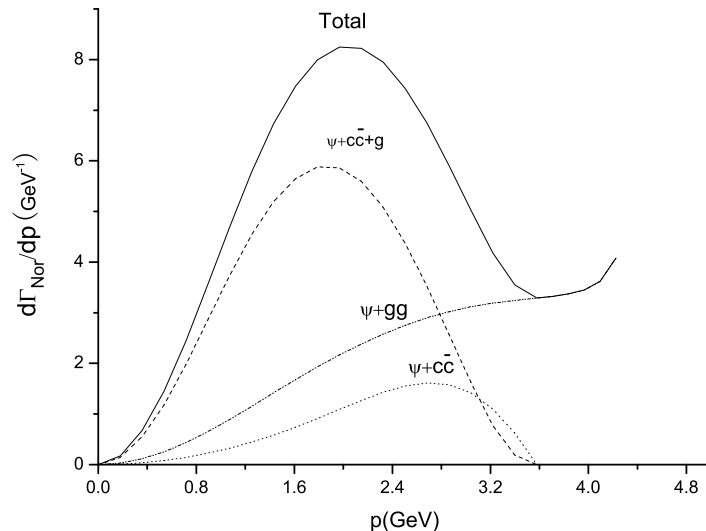


FIG. 3: The contributions of QCD process $\Upsilon \rightarrow J/\psi + c\bar{c} + g$ (dashed line) and QED processes $\Upsilon \rightarrow J/\psi + gg$ (dot-dashed line) and 5 times of $\Upsilon \rightarrow \gamma^* \rightarrow J/\psi + c\bar{c}$ (dotted line) to J/ψ momentum distribution for J/ψ production in Υ decay. And the sum of them is given by the solid line.

On the experimental side, the CLEO collaboration find[24] that the feed-down of χ_{cJ} to J/ψ are $< 8.2, 11, 10$ percent for $J = 0, 1, 2$ respectively and the feed-down of $\psi(2S)$ is about 24 percent in $\Upsilon \rightarrow J/\psi + X$. Therefore it indicates that the experimental result of direct J/ψ production would be

$$\mathcal{B}_{\text{Direct}}(\Upsilon \rightarrow J/\psi + X) = 3.52 \times 10^{-4} \quad (29)$$

which is about 9 times larger than the presented theoretical results based on the color-singlet calculations. This means that unlike the conclusion before[26] the branching ratio of $\Upsilon \rightarrow J/\psi + X$ can not be explained by color-singlet model at the leading order.

From the theoretical point of view, the color-octet mechanism can account for most J/ψ production, but its predictions for the J/ψ momentum spectrum is not agree with the experimental data. The color-singlet predictions on the shape of the J/ψ momentum spectrum is more closer to the experimental result, but the discrepancy of the branching ratio between them is large. For all the numerical results, we used the theoretically normalized decay width to estimate the branching ratio. Alternatively, by using $\langle \Upsilon | O_1(^3S_1) | \Upsilon \rangle = 2.9 \text{GeV}^3$ [20] to calculate the partial decay width and choosing the total decay width of

Υ 51.4 keV from the experimental measurement[34], the branching ratio will be enhanced by a factor of about 3, which still can not explain the experimental results. Therefore, it means that the NLO QCD correction is important, just like in the known cases, the NLO QCD corrections for J/ψ production in e^+e^- annihilation show that the K -factor are about 1.97 and 1.2 for $e^+e^- \rightarrow \gamma^* \rightarrow J/\psi + c\bar{c}$ and $e^+e^- \rightarrow \gamma^* \rightarrow J/\psi + gg$ processes respectively; the NLO QCD correction in J/ψ related Υ exclusive decays are also found quite important [35]. In addition, the contribution of $\mathcal{O}(\alpha_s^6)$ processes $b\bar{b}(^3S_1, 1) \rightarrow c\bar{c}(^3S_1, 1) + gg$ and $b\bar{b}(^3S_1, 1) \rightarrow c\bar{c}(^3S_1, 1) + gggg$ to the branching ratio has been estimated to be of 10^{-4} order[25]. So that the next important step is to give an explicit and complete calculations of them, which will be very helpful to understand the conflict between the theory and experiment. Furthermore, to obtain the full QCD correction for the inclusive J/ψ production in Υ decay would be a very interesting and challenge work for explaining the experimental data. But it will involve very complicated work at the QCD NLO and is beyond the scope of this work.

Acknowledgement

We thank Dr. S. Y. Li for helpful discussions. This work was supported by the National Natural Science Foundation of China (No. 10775141) and Chinese Academy of Sciences under Project No. KJCX3-SYW-N2. Zhiguo He is currently supported by the CPAN08-PD14 contract of the CSD2007-00042 Consolider-Ingenio 2010 program, and by the FPA2007-66665-C02-01/ project (Spain).

-
- [1] N. Brambilla *et al.* [Quarkonium Working Group], [arXiv:hep-ph/0412158].
 - [2] G. T. Bodwin, E. Braaten and G. P. Lepage, Phys. Rev. D **51**, 1125 (1995) [Erratum-ibid. D **55**, 5853 (1997)] [arXiv:hep-ph/9407339].
 - [3] F. Abe *et al.* [CDF Collaboration], Phys. Rev. Lett. **69**, 3704 (1992).
 - [4] E. Braaten and S. Fleming, Phys. Rev. Lett. **74**, 3327 (1995) [arXiv:hep-ph/9411365].
 - [5] A. A. Affolder *et al.* [CDF Collaboration], Phys. Rev. Lett. **85**, 2886 (2000).
 - [6] B. Gong, X. Q. Li and J. X. Wang, Phys. Lett. B **673**, 197 (2009).

- [7] J. M. Campbell, F. Maltoni and F. Tramontano, Phys. Rev. Lett. **98**, 252002 (2007) [arXiv:hep-ph/0703113]; B. Gong and J. X. Wang, Phys. Rev. Lett. **100**, 232001 (2008) [arXiv:0802.3727 [hep-ph]]; B. Gong and J. X. Wang, Phys. Rev. D **78**, 074011 (2008) [arXiv:0805.2469 [hep-ph]].
- [8] P. Artoisenet, J. M. Campbell, J. P. Lansberg, F. Maltoni and F. Tramontano, Phys. Rev. Lett. **101**, 152001 (2008) [arXiv:0806.3282 [hep-ph]].
- [9] D. E. Acosta *et al.* [CDF Collaboration], Phys. Rev. Lett. **88**, 161802 (2002).
- [10] V. M. Abazov *et al.* [D0 Collaboration], Phys. Rev. Lett. **101**, 182004 (2008) [arXiv:0804.2799 [hep-ex]].
- [11] E. Braaten and Y. Q. Chen, Phys. Rev. Lett. **76**, 730 (1996) [arXiv:hep-ph/9508373]; F. Yuan, C. F. Qiao and K. T. Chao, Phys. Rev. D **56**, 321 (1997) [arXiv:hep-ph/9703438].
- [12] B. Aubert *et al.* [BABAR Collaboration], Phys. Rev. Lett. **87**, 162002 (2001) [arXiv:hep-ex/0106044].
- [13] K. Abe *et al.* [BELLE Collaboration], Phys. Rev. Lett. **88**, 052001 (2002) [arXiv:hep-ex/0110012].
- [14] S. Fleming, A. K. Leibovich and T. Mehen, Phys. Rev. D **68**, 094011 (2003) [arXiv:hep-ph/0306139].
- [15] K. Abe *et al.* [Belle Collaboration], Phys. Rev. Lett. **89**, 142001 (2002) [arXiv:hep-ex/0205104]. P. Pakhlov *et al.* [Belle Collaboration], arXiv:0901.2775 [hep-ex].
- [16] Y. J. Zhang, Y. j. Gao and K. T. Chao, Phys. Rev. Lett. **96**, 092001 (2006) [arXiv:hep-ph/0506076].
- [17] B. Gong and J. X. Wang, Phys. Rev. D **80**, 054015 (2009) arXiv:0904.1103 [hep-ph].
- [18] Y. Q. Ma, Y. J. Zhang and K. T. Chao, Phys. Rev. Lett. **102**, 162002 (2009) [arXiv:0812.5106 [hep-ph]].
- [19] B. Gong and J. X. Wang, Phys. Rev. Lett. **102**, 162003 (2009) [arXiv:0901.0117 [hep-ph]];
- [20] K. M. Cheung, W. Y. Keung and T. C. Yuan, Phys. Rev. D **54**, 929 (1996) [arXiv:hep-ph/9602423].
- [21] M. Napsuciale, Phys. Rev. D **57**, 5711 (1998) [arXiv:hep-ph/9710488].
- [22] R. Fulton *et al.* [CLEO Collaboration], Phys. Lett. B **224**, 445 (1989).
- [23] H. Albrecht *et al.* [ARGUS Collaboration], Z. Phys. C **55**, 25 (1992).
- [24] R. A. Briere *et al.* [CLEO Collaboration], Phys. Rev. D **70**, 072001 (2004)

- [arXiv:hep-ex/0407030].
- [25] H. D. Trottier, Phys. Lett. B **320**, 145 (1994) [arXiv:hep-ph/9307315].
- [26] S. Y. Li, Q. B. Xie and Q. Wang, Phys. Lett. B **482**, 65 (2000) [arXiv:hep-ph/9912328];
W. Han and S. Y. Li, Phys. Rev. D **74**, 117502 (2006) [arXiv:hep-ph/0607251].
- [27] H. Fritzsch and K. H. Streng, Phys. Lett. B **77**, 299 (1978).
- [28] I. I. Y. Bigi and S. Nussinov, Phys. Lett. B **82**, 281 (1979).
- [29] J. H. Kuhn, J. Kaplan and E. G. O. Safiani, Nucl. Phys. B **157**, 125 (1979). B. Guberina,
J. H. Kuhn, R. D. Peccei and R. Ruckl, Nucl. Phys. B **174**, 317 (1980).
- [30] P. L. Cho and A. K. Leibovich, Phys. Rev. D **53**, 150 (1996) [arXiv:hep-ph/9505329];
P. L. Cho and A. K. Leibovich, Phys. Rev. D **53**, 6203 (1996) [arXiv:hep-ph/9511315]; P. Ko,
J. Lee and H. S. Song, Phys. Rev. D **54**, 4312 (1996) [Erratum-ibid. D **60**, 119902 (1999)]
[arXiv:hep-ph/9602223].
- [31] J.-X. Wang, Nucl. Instrum. Meth. A **534**, 241 (2004).
- [32] E. J. Eichten and C. Quigg, Phys. Rev. D **52**, 1726 (1995) [arXiv:hep-ph/9503356].
- [33] Z. H. Lin and G. h. Zhu, Phys. Lett. B **597**, 382 (2004) [arXiv:hep-ph/0406121].
- [34] C. Amsler *et al.* [Particle Data Group], Phys. Lett. B **667**, 1 (2008).
- [35] G. Hao, Y. Jia, C. F. Qiao and P. Sun, JHEP **0702**, 057 (2007) [arXiv:hep-ph/0612173].
B. Gong, Y. Jia and J. X. Wang, Phys. Lett. B **670**, 350 (2009) [arXiv:0808.1034 [hep-ph]].